Rationale Behind EU-DEMO Limiter's Plasma-Facing Component Design Under Material Phase Change

M. L. Richiusa, P. Ireland, J. Nicholas, and Z. Vizvary

***Abstract*— The protection strategy adopted for the European DEMOnstration (EU-DEMO) fusion power reactor foresees the use of sacrificial components–referred to as limiters–dealing with plasma-wall contacts. Their aim is to protect the first wall (FW) against the huge amount of plasma energy (up to GigaJoules) released in a few milliseconds during disruptive events, which might lead to melting and/or vaporization of the foreseen plasma-facing tungsten armor. The current limiter design concepts rely on actively water-cooled plasma-facing components (PFCs) made of tungsten. As water is not allowed inside the main chamber, limiter's PFCs must be designed to preserve the cooling system integrity under any scenario, therefore the estimate of the thickness of material undergoing any phase change is crucial. Given the initial assessment of plasma magnetic configurations during off-normal events, this article describes the procedure followed for designing the limiter's PFC, which includes a novel approach for estimating the molten thickness of material under high heat flux. A simplified 1-D model has been implemented in MATLAB, which deals with multiphase moving boundary problems, hence its name Thermal Analysis foR Tracking InterFaces under meLting&vaporizaTion-induced plasma Transient Events (TARTIFL&TTE). This model takes its inspiration from the way phase change interface tracking problems are tackled in food industry (i.e., freeze-drying processes) and solute concentration diffusion-controlled problems. It overcomes the complexity of solving a strongly coupled non-linear system of partial and ordinary differential equations in moving spatial domains by adopting a change of coordinate system based on the Landau transformation. As a result, an equivalent and fixed spatial coordinate system is defined where the spatial domain boundaries of the different phases are constrained, and the systems of governing equations are easy to solve. Both the solid and liquid phases are modeled, while the vapor is assumed to be removed once formed. Its benchmark against computational results found in the literature has shown a very good agreement, which paves the way to further development of it. For phase change interface tracking problems in 2-D/3-D and more complex geometries, a commercial Multiphysics software adopting the Lagrangian–Eulerian approach in moving mesh frames will be used for tackling problems where material is removed following a phase change. Although the vapor domain is not simulated, a set of gas kinetics boundary conditions couples the interface between vapor and liquid phases, driving its position over time. This will be detailed described in a future companion article.**

***Index Terms*— Design methodology, fusion power generation, tokamaks.**

Manuscript received 29 December 2021; revised 30 March 2022; accepted 9 April 2022. Date of publication 11 May 2022; date of current version 30 November 2022. This work was supported in part by the EUROfusion Consortium and in part by the Euratom Research and Training Program 2014–2018 and 2019–2020 under Grant 633053. The review of this article was arranged by Senior Editor G. H. Neilson. *(Corresponding author: M. L. Richiusa.)*

M. L. Richiusa is with the Department of Engineering Science, Oxford Thermofluids Institute, University of Oxford, Oxford, OX2 0ES, U.K., and also with the UKAEA-CCFE, Culham Science Centre, Abingdon OX14 3DB, U.K. (e-mail: lorena.richiusa@ukaea.uk).

P. Ireland and J. Nicholas are with the Oxford Thermofluids Institute, University of Oxford, Oxford, OX2 0ES, U.K.

Z. Vizvary is with the UKAEA-CCFE, Culham Science Centre, Abingdon OX14 3DB, U.K.

Color versions of one or more figures in this article are available at https://doi.org/10.1109/TPS.2022.3169232.

Digital Object Identifier 10.1109/TPS.2022.3169232

NOMENCLATURE

Acronyms

CQ	Current quench.
DVDE	Downward vertical displacement event.
DEMO	DEMOnstration fusion power plant.
FW	First wall.
OLL	Outboard lower limiter.
OML	Outboard midplane limiter.
PDE	Partial differential equation.
PFC	Plasma-facing component.
RU/RD	Ramp-up/ramp-down.
SOF	Start-of-flat top.
SOL	Scrape-off layer.
TQ	Thermal quench.
UL	Upper limiter.
UVDE	Upper vertical displacement event.

Symbols

c_p	Specific heat capacity, [J · kg^{-1} · K^{-1}].
f	Function describing the PFC toroidal profile.
H	Latent heat, [J · m^{-3}].
k	Thermal conductivity, [W · m^{-1} · K^{-1}].
L	Characteristic width, [m].
q	Heat flux, [W · m^{-2}].
r	Liquid/vapor moving interface position, [m].
s	Solid/liquid moving interface position, [m].
t	Time, [s].
T	Temperature, [°C].
W	Tungsten.
x	Current spacial coordinate, [m].

Subscripts

l	Liquid.
m	Melting.

max	Maximum.
op	Operational.
s	Solid.
v	Vapor.

Greek

ζ	Vapor phase domain spatial coordinate, [m].
η	Solid phase domain spatial coordinate, [m].
ϕ	Toroidal coordinate.
ξ	Liquid phase domain spatial coordinate, [m].
ρ	Density, [kg $\cdot$ m^{-3}].
λ	SOL power fall-off decay length, [m].

I. Introduction

TOGETHER with plasma disruption mitigation strategies, special requirements are needed for preventing the plasma from touching the wall during both normal and disruptive events in future tokamaks. Unlike the existing experimental tokamaks, which work either without tritium or with lower plasma power levels, DEMO cannot operate safely with a bare tritium-breeding wall [1] as any plasma major perturbation could push its boundary toward the wall that will be severely damaged. Therefore, protruding protection panels (aka limiters), discrete along both the poloidal and toroidal directions, will be used for constraining the plasma boundaries.

Plasma-facing materials should cope with high heat fluxes under neutron irradiation, minimizing the influx of impurities into the plasma, the tritium trapping, and its neutron activation level. The EU-DEMO wall will be made of W-coated EUROFER as structural material for the breeding blanket, whereas the divertor will foresee actively cooled W monoblocks. Limiters can be thought as components made up of an actively water-cooled W mono-block PFC, which is attached to an actively water-cooled EUROFER shield block directly fastened to the vacuum vessel. This means that limiters are going to replace the breeding blanket in the poloidal and toroidal locations where they are needed.

Limiters do not play any role in plasma stability. They are only meant to face plasma-wall impacts following unmitigated perturbations, which have been simulated by assuming a toroidal symmetry of the 2-D plasma equilibrium. Four different limiters are required to adequately protect the FW (see Fig. 2 in [1]) of the EU-DEMO 2017 baseline:

1) OML (four in the 360° torus) for plasma RU/RD phases (see Fig. 3 in [2] for magnetic equilibrium shape), and located at the outboard mid-plane. Plasma parameters: $P_{\mathrm{SOL}} = 3.5$ MW in 35 s, $\lambda = 6$ mm;
2) OLL (four in total) facing DVDEs (see Fig. 5 (lhs) in [2] for magnetic equilibrium shape) following vertical instabilities (caused by current or voltage value deviations from their reference ones), during which the plasma loses energy (TQ) while moving downward, for then experiencing a CQ before disappearing. Plasma parameters during TQ: $P_{\mathrm{SOL}} = 325$ GW in 4 ms, $\lambda = 7$ mm;

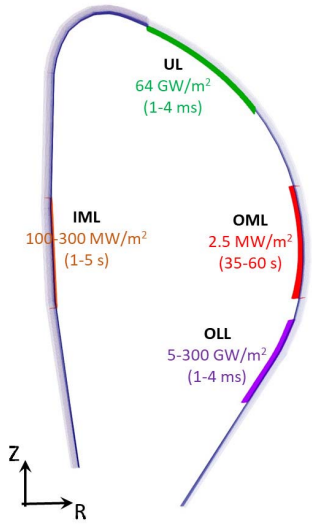

Fig. 1. Limiter heat load calculations due to charged particles during different plasma transients.

3) UL (eight in total) facing UVDEs (see Fig. 2 in [2] for magnetic equilibrium shape). Plasma parameters during TQ: $P_{\mathrm{SOL}} = 325$ GW in 4 ms, $\lambda = 7$ mm;
4) IML (four in total) facing other unforeseen transient events and H-L transitions (i.e., going from high to low plasma performances, see Fig. 5 (rhs) in [2] for magnetic equilibrium shape). Plasma parameters: $P_{\mathrm{SOL}} = 30$ MW in 5 s, $\lambda = 2$–4 mm.

During normal operation (i.e., Start-of-flat top, SOF—see Fig. 4 (rhs) in [1] for plasma equilibrium shape), the plasma is kept 225-mm away from the FW. A detailed description of the EU-DEMO 2017 Baseline plasma physics behind the definition of the magnetic equilibria can be found in Table I in [3].

The limiter location overview is sketched in Fig. 1 for a 2-D DEMO FW cross section, together with a summary of the charged particle maximum heat flux (q_{max}) experienced by every limiter during the related transient, along with its exposure time.

Having given an overview on the European DEMO protection strategy, the present article will briefly describe the work carried out for shaping the limiter plasma-facing surface in Section II, before focusing on the approach adopted for phase change material thickness estimate to be included in the engineering design (see Section III-A). The resulting thermal model, with its analytical formulation, benchmark, and application, will be described and discussed in Section III-A1.

II. Limiter Plasma-Facing Surface Shaping

As plasma-surface interactions are hence concentrated on the limiter's plasma-wetted surface, they need to be suitably and safely designed for withstanding different loading conditions.

Although they are primarily designed for facing off-normal transients, edge-localized power deposition peaks should be avoided during the longest SOF. Because of the different

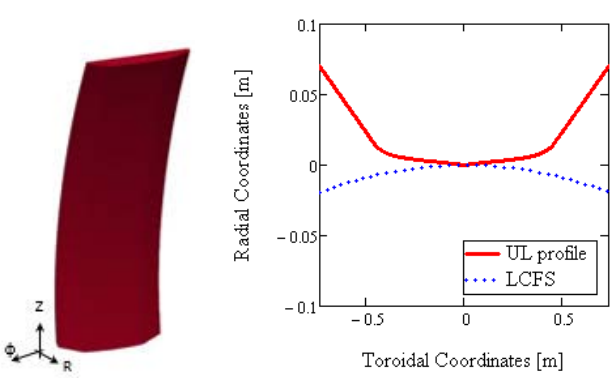

Fig. 2. UL plasma-facing surface (lhs) and its related toroidal 2shape profile (rhs).

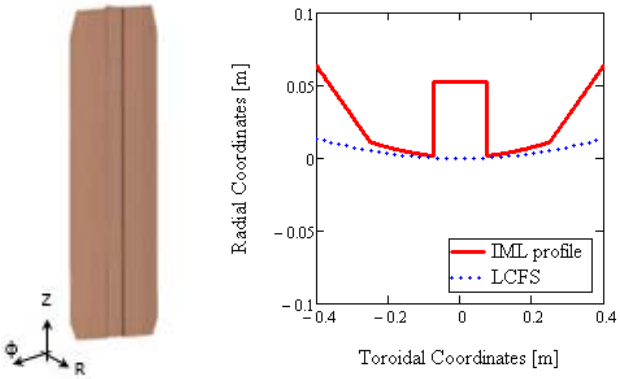

Fig. 4. IML plasma-facing surface (lhs) and its toroidal 2shape profile (rhs).

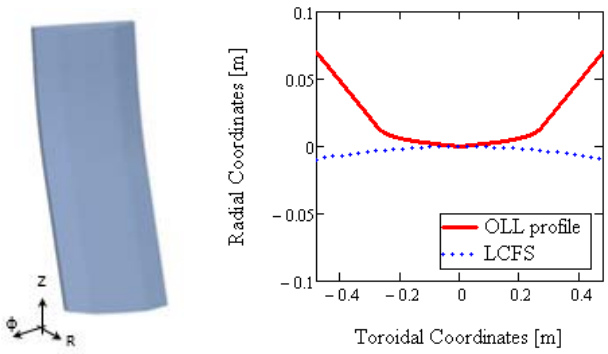

Fig. 3. OLL plasma-facing surface (lhs) and its toroidal 2shape profile (rhs).

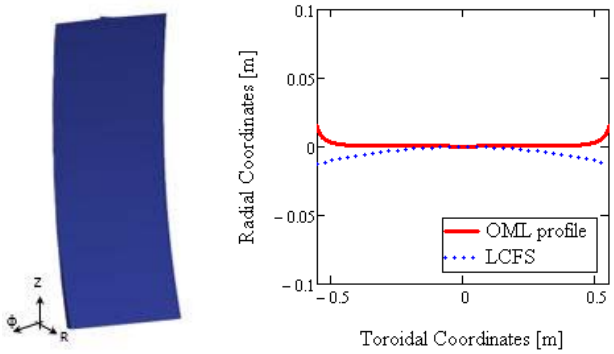

Fig. 5. OML plasma-facing surface (lhs) and its related toroidal profile (rhs).

plasma magnetic configurations [2], finding a unique surface shaping spreading the power deposition—due to charged particles spiraling along magnetic field lines—as even as possible during both SOF and transients is not straightforward, as the power deposition is described by an exponential law whose fall-off decay length is determined by λ. Hence, $q_{\max}$ moves from the center of the surface (due to smaller λ values during disruptions) to the edges (for larger λ during SOF—see Section I).

Each limiter's front face has been designed by starting from a similar approach than the one used for ITER FW shaping [4]. By imposing the following Cauchy problem, a mid-plane toroidal logarithmic profile $f(\phi)$ spreading the power deposition on as a large area as possible has been calculated for every component:

$$f(0) = 0 \tag{1}$$

$$e^{-\frac{f(\phi)}{\lambda}} \cdot f'(\phi) = \text{Constant}. \tag{2}$$

The initial condition on $f(\phi)$ imposes a distance between plasma and PFC equal to zero, and this point is used as the origin of a convenient rectilinear coordinate system defined for this calculation, whose radial direction is pointing into the surface, while the toroidal and poloidal ones are aligned with the global coordinate system. This contact point can be easily identified in the graphs plotted in Figs. 2–5. The second equation imposes a uniform constant power density value on the PFC toroidal profile, which will be eventually extruded along the poloidal length of the PFC.

The resulting logarithmic profile has been then adapted to the SOF magnetic configuration, by acting on the field-lines impinging angle. As a result of this iterative procedure carried out by means of field-lines tracing code SMARDDA [5], chamfers have been implemented to the analytical shaping function of UL, OLL, and IML, obtaining the so-called 2shape profile (see Figs. 2–4). Fig. 5 shows the OML untouched logarithmic profile, which has proved to be suitable for both RU and SOF equilibria under charged particle heat load calculation.

III. Plasma-Facing Material Challenges

A. Multiboundary Layer Approach for Heat Transfer Problems Involving Changes of Phase

Transient events can raise the temperature of the exposed surface up to the melting point and, eventually, to the boiling point. Metallic PFCs are prone to melting under heat loads in Fig. 1, which can cause erosion and reduction of the PFC lifetime. Hence, the molten material amount estimate should be design-driving and included somehow in the PFC finite element modeling and assessment.

The investigation of the heat transfer in solids involving a phase change falls within the Stefan-like problems [6], [7], which are characterized by interfaces between phases not known in advance. A moving interface is usually associated

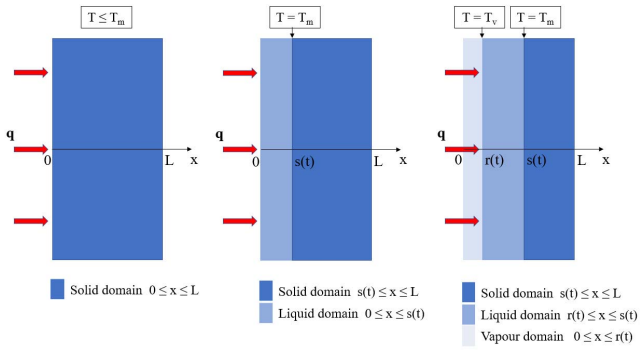

Fig. 6. Thermal model breakdown into the three main stages: heating up phase (lhs), melting phase (center) and vaporization phase (rhs).

with time-dependent heat conduction problems described by the Fourier equation, a set of initial and boundary equations, and an additional energy balance equation (i.e., Stefan condition) imposed at the interface between phases. Their resolution describes both the time and space temperature trends in all the phase domains and the evolution of the inter-phase boundary positions. The Stefan condition makes the PDE system strongly nonlinear as the time and space-evolution of the boundaries inherently depends on the calculated temperature. These problems are common in different research areas, i.e., casting solidification processes, food freezing, environmental engineering, ablation of missile skins under aerodynamic heating. Unfortunately, due to the nonlinearity of the problem, exact analytical solutions are limited to single moving boundary problems (i.e., one of the two phases stays at phase change temperature) where the thermal problem is solved for only one phase [8]. For multiple moving boundary problems, the solution has to be found numerically.

For a zero-order estimate of the molten layer, the Thermal Analysis foR Tracking InterFaces under meLting&vaporizaTion-induced plasma Transient Events (TARTIFL&TTE) software has been set up in MATLAB solving the three different stages of heat transfer highlighted in Fig. 6. A constant heat flux q is applied at one face of a finite slab which is initially at uniform temperature below the melting point, whereas its back face is insulated.

TARTIFL&TTE follows a staged-approach. The temperature rise is modeled until its front face reaches the melting point (triggering the beginning of the melting phase) and, eventually, the boiling point (beginning of the vaporization phase). The temperature distribution in the melted and unmelted portions of the slab, as well as the propagation of the melting layer, is therefore calculated.

1) Thermal Model Description: For simplifying the problem, the following assumptions are made.

1) The solid material is considered to be pure, and the temperature at the interfaces is assumed constant and equal to the temperature of the phase changes (see Fig. 6).
2) The solid is initially assumed to be at its isothermal temperature (T_{op}).
3) Material properties are assumed constant within every phase but different between different phases.
4) The vapor phase is assumed to be removed, once it appears. This means that the incoming heat flux is not absorbed by the vapor layer developed in front of the component, and hence no vapor shielding effect is here considered.
5) Additional parameters are: 1) L: sample width; 2) k_s, k_l: solid and liquid phases thermal conductivity; 3) cp: solid and liquid phases specific heat capacity; and 4) H_m, H_v: latent heat of fusion and vaporization, respectively.

Three different systems of PDEs are solved for the three different stages as follows.

1) *Heating Up Phase ($0 \le t \le t_m$):*
   a) Temperature values in the range $T_{\text{op}} \le T \le T_m$.
   b) Spatial domain of the solid phase $0 \le x \le L$.

   The governing Fourier equation is

$$k_s \frac{\partial^2 T_s(x,t)}{\partial x^2} = \rho c_p \frac{\partial T_s(x,t)}{\partial t} \tag{3}$$

   with the following initial and boundary conditions:

$$T(x,0) = T_{\text{op}} \tag{4}$$

$$k_s \frac{\partial T_s}{\partial x}\bigg|_{x=0} = -q \tag{5}$$

$$k_s \frac{\partial T_s}{\partial x}\bigg|_{x=L} = 0. \tag{6}$$

2) *Melting Phase ($t_m \le t < t_v$):*
   a) Temperature values in the range $T_m \le T \le T_v$.
   b) Two spatial domains: 1) liquid $0 \le x \le s(t)$ and 2) solid $s(t) \le x \le L$. This implies a solid-to-liquid interface moving boundary $s(t)$.

   The governing system of PDEs is

$$k_l \frac{\partial^2 T_l(x,t)}{\partial x^2} = \rho c_p \frac{\partial T_l(x,t)}{\partial t} \quad @ \quad 0 < x < s(t) \tag{7}$$

$$k_s \frac{\partial^2 T_s(x,t)}{\partial x^2} = \rho c_p \frac{\partial T_s(x,t)}{\partial t} \quad @ \quad s(t) < x < L. \tag{8}$$

   Considering the initial spatial temperature distribution the same as the one resulting from the heating up phase (see the following equation), the following initial conditions apply:

$$T_s(x,t_m) = T(x,t_m) \tag{9}$$

$$T_s(0,t_m) = T_m \tag{10}$$

$$s(t_m) = 0 \tag{11}$$

   together with the boundary conditions

$$-k_l \frac{\partial T_l}{\partial x}\bigg|_{x=s(t)} + k_s \frac{\partial T_s}{\partial x}\bigg|_{x=s(t)} = \rho H_m \frac{ds(t)}{dt} \tag{12}$$

$$T_s(s(t),t) = T_l(s(t),t) = T_m \tag{13}$$

$$k_l \frac{\partial T_l}{\partial x}\bigg|_{x=0} = -q. \tag{14}$$

3) *Vaporization Phase ($t \geq t_v$):*
   a) Temperature values in the range $T \leq T_v$.
   b) Three spatial domains: 1) vapor $0 \leq x \leq r(t)$; 2) liquid $r(t) \leq x \leq s(t)$; and 3) solid $s(t) \leq x \leq L$. Two different interfaces are considered, i.e., vapor-to-liquid $r(t)$ and solid-to-liquid $s(t)$ moving boundaries.

The governing system of PDEs is the following:

$$k_l \frac{\partial^2 T_l(x,t)}{\partial x^2} = \rho c_p \frac{\partial T_l(x,t)}{\partial t} \quad @ \quad r(t) < x < s(t) \tag{15}$$

$$k_s \frac{\partial^2 T_s(x,t)}{\partial x^2} = \rho c_p \frac{\partial T_s(x,t)}{\partial t} \quad @ \quad s(t) < x < L \tag{16}$$

with the initial conditions listed below (by assuming the initial temperature distribution of the solid and liquid domains are the same as the ones resulting from the melting phase, i.e., (17) and (18), respectively)

$$T_s(x,t_v) = T(x,t_v) \tag{17}$$

$$T_l(x,t_v) = T(x,t_v) \tag{18}$$

$$r(t_v) = 0 \tag{19}$$

$$s(t_v) = s(t) \tag{20}$$

$$T_l(0,t_v) = T_v \tag{21}$$

and the following boundary conditions:

$$q + k_l \frac{\partial T_l}{\partial x}\bigg|_{x=r(t)} = \rho H_v \frac{dr(t)}{dt} \tag{22}$$

$$-k_l \frac{\partial T_l}{\partial x}\bigg|_{x=s(t)} + k_s \frac{\partial T_s}{\partial x}\bigg|_{x=s(t)} = \rho H_m \frac{ds(t)}{dt} \tag{23}$$

$$T_v(r(t),t) = T_l(r(t),t) = T_v \tag{24}$$

$$T_s(s(t),t) = T_l(s(t),t) = T_m. \tag{25}$$

Taking into account moving boundary problems faced in freeze-drying [9] and solute concentration diffusion-controlled [10] processes, the Landau approach [11] simplifies the computational resolution of the problem. This is based on a transformation of the coordinate system by defining spatial variables (one for each phase) which, in turn, depend upon the moving interface. Although the transformation adds an additional complication inside the Fourier equation defined in every domain, it spatially constraints the phase domains between [0, 1]. Furthermore, their related spatial discretization takes into account the motion of the interface, which always falls in points where it is actually calculated. Consequently, any of the numerical methods developed to solve systems of PDEs can be used for solving the problem.

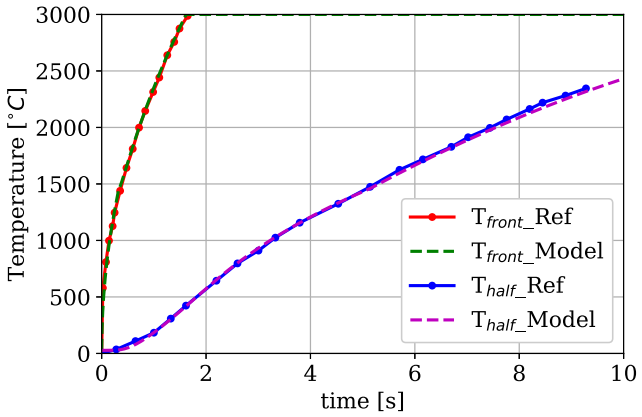

Fig. 7. Temperature evolution at the front face and at half thickness ($L/2$) of the 1-D model.

The transformation introduces the following new spatial variables, which transform the PDEs listed above accordingly:

$$\text{vapor domain: } \zeta = \frac{x}{r(t)} \quad \Rightarrow \quad 0 \leq \zeta \leq 1 \tag{26}$$

$$\text{liquid domain: } \xi = \frac{x - r(t)}{s(t) - r(t)} \quad \Rightarrow \quad 0 \leq \xi \leq 1 \tag{27}$$

$$\text{solid domain: } \eta = \frac{x - s(t)}{L - s(t)} \quad \Rightarrow \quad 0 \leq \eta \leq 1. \tag{28}$$

2) Computational Benchmark: TARTIFL&TTE has been benchmarked against the results related to (a) heat transfer problem involving heating and complete collapse of a solid wall through melting and (b) heat transfer problem involving melting and partial vaporization of the liquid in [12]. The authors in [12] compare different algorithms (finite elements, finite differences, boundary elements) for solving the same multiphase moving boundary problems. For sake of brevity, the benchmark is shown only for the latter problem (b) [12], although both the cases have given very promising results in terms of temperature evolutions (see Fig. 7), inter-phase boundary positions (see Fig. 8) and velocities (see Fig. 9). Although the thermal model needs to be developed further, at this stage it has been applied for an estimate of the W molten thickness under heat loads generated by VDEs (see Fig. 1). In case of UVDE, a pure W slab undergoing a constant $q \approx 70$ GW/m^2 for 4 ms experiences an instantaneous rise of its surface temperature (see Fig. 10) up to the melting point (3422 °C in 0.42 μs), and, eventually, up to the boiling point (5660 °C in 2 μs), producing a final melt and vapor thicknesses of, respectively, 4.5 and 4 mm. The same sudden temperature rise trend occurs under DVDE heat loads, although the huge amount of energy deposited on the surface brings it to melting in 0.06 μs and vaporization in less than 1 μs. At the end of the transient, the depth of the molten layer is ≈18 mm, of which ≈17 mm are vaporized. Under DVDE, the vapor thickness may seem unrealistic since vapor shielding effects are not here considered, and therefore the total incoming heat

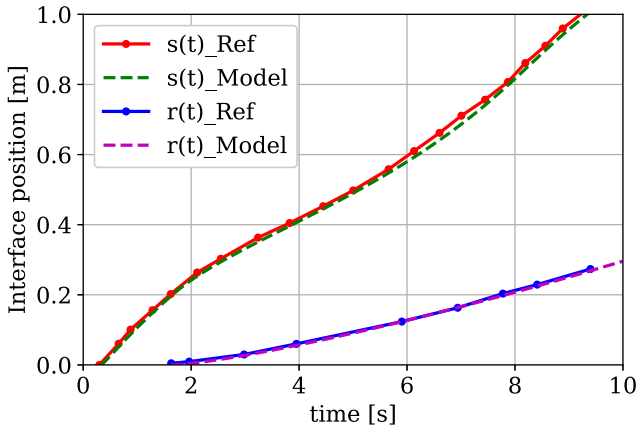

Fig. 8. Solid/liquid ($s(t)$) and liquid/vapor ($r(t)$) moving boundary tracking.

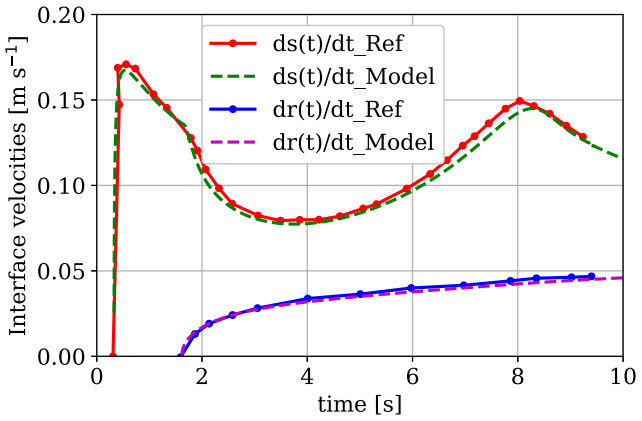

Fig. 9. Solid/liquid ($s(t)$) and liquid/vapor ($r(t)$) moving boundary velocities.

flux is absorbed by phase changes rather than shielded by the vapor layer, which would affect the energy balance. Therefore, the simulated cases seem to be the worst case scenarios. Based on these preliminary results, the zero-order MATLAB code predicts (at least) a 20-mm-thick W armor to face the critical plasma-surface impact during VDEs.

3) Result Discussion and Further Work: The results obtained under VDE heat loads might not be realistically catching the physics governing the intense evaporation under vacuum, for at least two reasons: 1) the model represents the first attempt to tackle these kinds of problems and 2) gas kinetics has not been taken into account in TARTIFL&TTE for describing the vaporization phase, which in its intense occurrence under vacuum conditions might not be well represented by a simple energy balance at the inter-phase. Despite this, the molten layer depth during UVDE appears to be of the same order of magnitude than the estimated molten thickness of $\approx$1100 μm in [13]. Hence, there is the need to validate this approach against experimental results. The temperature evolution in Fig. 10 clearly shows that fast transients only affect the PFC surface. The TQ time scale is too short for letting the heat to diffuse across the sample thickness, therefore the PFC outermost layers only face the thermal wave by means of their material thermal inertia, leaving the rest of it at T_{op}.

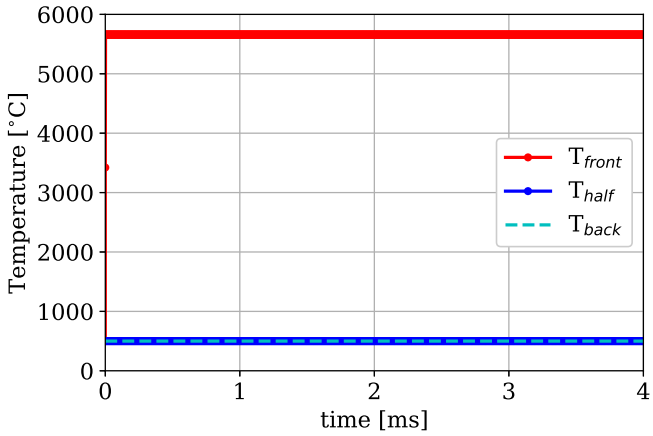

Fig. 10. Temperature evolution in a 1-D finite slab of pure W withstanding the heat flux of a UVDE/DVDE.

Provided that the molten thickness estimate is acceptable, this means that any cooling system located at least 20 mm far from the PFC surface should be considered unperturbed by the disruptive event. The Landau transformation is an easy way of overcoming the more complicated Lagrangian–Eulerian approach to the moving boundary problems, which require both more coding and computational efforts. The computational benchmark at low power level is promising, and it encourages a further development of the TARTIFL&TTE approach after a deep dig on how the vaporization affects the heat transfer on the condensed phase, and whether any vapor shielding effects should be considered in the total amount of energy diffused across it. For the sake of improving the knowledge gained so far, parallel studies on the two above-mentioned points are currently carried on by the aid of a Multiphysics software, and experiment planning is an additional feature which will help broaden the understanding on this topic. This will be illustrated in a future companion article.

IV. Conclusion

Within the framework of EUROfusion DEMO FW and limiter design activities, the protection of the FW against power deposition peaks is one of the main criteria driving its design. Limiters are foreseen as sacrificial components for withstanding high heat fluxes following plasma-wall contacts in short timescale, preventing any FW irreversible damage. This feature makes the limiter design even more challenging as it should tackle non-conventional issues. If the shaping of their front face is needed for accommodating heat loads coming from different plasma magnetic scenarios, i.e., both off-normal transients and normal operations, the estimate of the potential melting depth is important for safety requirements raised by any water leakage inside the main vacuum chamber. Therefore, the integrity of the limiter cooling system should always been ensured. The aim of the present study is how the melting and vaporization erosion effects might be approached inside the design of a metallic PFC (especially limiters but easily extended to any PFC) directly exposed to

plasma impact. It has appeared sensible tackling the issue as a multiphase moving boundary problem, which is complicated by the appearance of interfaces whose movement is energy balance-driven. The way the thermal problem has been approached, and implemented in MATLAB, has brought to the creation of the TARTIFL&TTE software. It takes the idea from the way the moving boundary problems are tackled in other technological processes (i.e., freeze-drying, solute concentration diffusion etc.). The benchmark against data found in literature about the collapse of a slab under melting and partial vaporization under low/moderate heat loads encourages a further development of it. No gas kinetics has been included at this stage. When applied to a W PFC withstanding heat loads typical of a DVDE, the zero-order MATLAB code predicts a depth of 20 mm (at least) far away from the irradiated surface, where the cooling system could be potentially considered safe, although the physics behind vaporization and the way it affects the energy balance needs a better understanding and implementation. The ongoing work is moving toward this direction, by looking at both the computational Lagrangian-Eulerian approach already implemented in Multiphysics software and experimental feedback, and the next step development will be explained in a future companion article.

ACKNOWLEDGMENT

The views and opinions expressed herein do not necessarily reflect those of the European Commission.

REFERENCES

[1] M. L. Richiusa *et al.*, "Bare and limiter DEMO single module segment concept first Wall misalignment study by 3D field line tracing," *Fusion Eng. Des.*, vol. 160, Nov. 2020, Art. no. 111839.

[2] F. Maviglia *et al.*, "Impact of plasma thermal transients on the design of the EU DEMO first wall protection," *Fusion Eng. Des.*, vol. 158, Sep. 2020, Art. no. 111713.

[3] M. Siccinio *et al.*, "Development of the plasma scenario for EU-DEMO: Status and plans," *Fusion Eng. Des.*, vol. 176, Mar. 2022, Art. no. 113047.

[4] P. C. Stangeby and R. Mitteau, "Analysis for shaping the ITER first wall," *J. Nucl. Mater.*, vol. 390, no. 1, pp. 963–966, 2009.

[5] W. Arter, V. Riccardo, and G. Fishpool, "A CAD-based tool for calculating power deposition on tokamak plasma-facing components," *IEEE Trans. Plasma Sci.*, vol. 42, no. 7, pp. 1932–1942, Jul. 2014.

[6] H. S. Carslaw and J. C. Jaeger, *Conduction of Heat in Solid*. Oxford, U.K.: Clarendon Press, 1986.

[7] J. Crank, *Free and Moving Boundary Problems*. Oxford, U.K.: Clarendon Press, 1987.

[8] H. Hu and S. A. Argyropoulos, "Mathematical modelling of solidification and melting: A review," *Model. Simul. Mater. Sci. Eng.*, vol. 4, no. 4, pp. 371–396, 1996.

[9] C. Vilas, A. A. Alonso, E. Balsa-Canto, E. Lopez–Quiroga, and I. C. Trelea, "Model-based real time operation of the freeze-drying process," *Processes*, vol. 8, no. 3, p. 325, 2020.

[10] T. C. Illingworth and I. O. Golosnoy, "Numerical solutions of diffusion-controlled moving boundary problems which conserve solute," *J. Comput. Phys.*, vol. 209, no. 1, pp. 207–225, 2005.

[11] H. G. Landau, "Heat conduction in a melting solid," *Quart. Appl. Math.*, vol. 8, no. 1, pp. 81–94, 1950.

[12] M. Zerroukat and C. R. Chatwin, *Computational Moving Boundary Problems* (Applied and Engineering Mathematics Series). Boston, MA, USA: Research Studies Press, 1994.

[13] F. Maviglia *et al.*, "Integrated design strategy for EU-DEMO first wall protection from plasma transients," *Fusion Eng. Des.*, vol. 177, Apr. 2022, Art. no. 113067.